Electrochemical Modeling and Characterization of Voltage Operated Channels in Nano–Bio–Electronics

Massimo Longaretti[1], Bice Chini[2],

Joseph W. Jerome[3], Riccardo Sacco[4,*]

[1] Dipartimento di Matematica "F. Brioschi", Politecnico di Milano,

via Bonardi 9, 20133 Milano, Italy.

E-mail: massimo.longaretti@polimi.it.

[2] CNR Institute of Neuroscience Department of Pharmacology,

Università degli Studi di Milano,

via Vanvitelli 32, 20129 Milano, Italy.

Tel.: +39 02 5031 6958, E-mail: B.Chini@in.cnr.it.

[3] Department of Mathematics, Northwestern University,

2033 Sheridan Road, Evanston, IL 60208-2730, USA.

Tel.: +01 847 491 5575, E-mail: jwj@math.northwestern.edu.

[4] Dipartimento di Matematica "F. Brioschi", Politecnico di Milano,

via Bonardi 9, 20133 Milano, Italy.

Tel.: +39 02 2399 4540, E-mail: riccardo.sacco@polimi.it.

* Corresponding author.

Abstract

In this article, the electrical characterization of Voltage Operated ionic Channels (VOCs) in Nano–Bio–Electronics applications is carried out. This is one of the relevant steps towards a multi–physics description of hybrid bio–electronical devices such as bio–chips. Electrochemical ionic transport phenomena are properly modeled by a Poisson-Nernst-Planck partial differential system of nonlinearly coupled equations, while suitable functional iteration techniques for problem decoupling and finite element methods for discretization are proposed and discussed. Extensive numerical simulations of single species VOCs transporting K^+ ions are performed to consistently derive an electrical equivalent representation of the channel and to quantitatively describe its interaction with an external measurement device under several working conditions.

Keywords: Nanotechnology; hybrid bio–artificial systems; ElectroPhysiology; ionic–electrical coupling; ionic channels; mathematical modeling; numerical simulation.

1 Introduction and Motivations

The investigation and development of accurate measurement techniques and procedures for the experimental characterization of bio-cellular processes is a relevant and delicate issue. Some motivations for this statement are:

- the intrinsic complexity of the biological system, because of the simultaneous presence of several mutually interacting subsystems, such as ionic channels and ion transport pumps [6, 10], that cooperate to regulate and maintain the dynamical electro-chemical equilibrium between the cell surrounding environment and the intracellular *milieu* [1];
- the difficulty in the implementation of a tool that is capable to perform a *selective* activation of single subsystems and to function in a *local* manner, on the spatial scale of the subsystems themselves (nanometers), filtering out the background noise due to phenomena that occur on a macroscopic neighbourhood (micrometers) of the cellular membrane.

Several methodologies have been devised to reach a sufficient degree of accuracy for Electro-Physiology (EP) applications, among which we mention the Voltage-Clamp (VC) [9] and the Patch-Clamp (PC) [10, 9] techniques. The VC technique is the basic configuration tool for measurement in EP and is aimed at stabilizing the voltage drop across the membrane in order to obtain an accurate current-voltage characterization of the biological system. The VC technique allows to selectively activate biological transmission mechanisms through the use of specific pharmacological tools, but it is not able to solve the background noise problem. The PC technique represents the most advanced level in measurement in EP, thanks to a highly sophisticated design of the instrumentation equipment which allows to detect single biological devices (ionic channel) and to electrically isolate them from the neighbouring environment. The PC technique is thus able to overcome the background noise problem affecting the VC technique,

and the continuous improvement of its implementation and performance has been the main technological supporting tool for the experimental scientifical activity that made it possible for E. Neher and B. Sakmann to win the Nobel Prize for Medicine in 1991 "*for their discoveries concerning the function of single ion channels in cells*".

Despite the substantial progress in EP measurement procedures, the several biological, experimental and technological difficulties described above become further amplified when the focus of the application is to design and devise a mutual interaction of electrical type between a biological system and an integrated chip, realized according to a standard silicon-based planar technology. An example of this ambitious task, which represents one of the critical step in Bio-Nano-Electronics applications, is the bio-hybrid EOSFET (Electrolyte Oxide Semiconductor Field Effect Transistor) device thoroughly discussed and investigated in [16, 19, 5] and more recently object of extensive numerical analysis in [12, 13].

Mathematical modeling, combined with robust and efficient computational tools, can provide a valid support to experimental procedures, because it allows to establish a rigorous and quantitative relation between the *measurable* information of physical interest (ionic current fluxes, membrane potential transients, action potentials) and the corresponding *biological* underlying mechanisms. In particular, a sound and accurate mathematical description of the problem makes it possible to distinguish the contribution to the measured quantity due to the intrinsic dynamics of the system from the (unavoidable) perturbations due to the experimental equipment.

In the present article, we have the following objectives:

- to characterize a single-species voltage operated ionic channel (VOC) transporting K^+ ions through the adoption of an established model based on partial differential equations (PDE) such as the *Poisson-Nernst-Planck* (PNP) system. For this purpose, we employ suitable and effective functional iteration procedures for the linearization of the PNP

model, combined with accurate and stable numerical schemes for its temporal and spatial discretization;

- to describe the interaction between the single ionic channel and the measurement system through the coupling of the PNP model with a reduced–order model based on ordinary differential equations (ODE) and characterized by the introduction of suitable lumped electrical equivalent parameters that represent the non-ideal effects and limitations of the instrumentation equipment;

- to perform a preliminary study of the effects related to a multi-channel stimulation, under the simplifying assumption that the involved channels share the same structure, morphology and functional behaviour.

A summary of the contents of the article is as follows. In Sect. 2 we provide a schematical description of a current-voltage measurement tool based on the VC technique, and we address the need of performing a coupled multi-physics PDE/ODE model in order to end up with a quantitatively accurate description of the system at the expense of a computationally affordable simulation. In Sect. 3 we discuss in detail the PNP model for electrochemical charge transport in a VOC, while in Sect. 4 we illustrate the functional and numerical techniques adopted for linearization and discretization. Finally, in Sect. 5 we demonstrate the physical validity of the model and the accuracy of computational techniques, on the numerical simulation of a measurement system in the case of a single-channel and multi-channel configuration under several working conditions. Some concluding remarks and future research directions are addressed in Sect. 6.

2 Schematic Description of A Current-Voltage Measurement Tool For VOCs

In this section, we provide a schematic description of a typical voltage–current measurement tool in ElectroPhysiology applications, based on the VC technique introduced in Sect. 1. For further details and information, we refer to [6, 1].

In Fig. 1, we show the electrical voltage stimulator V_{st} (assumed to be lossless) and a two-dimensional cross–section of the cellular membrane (shaded area) where a number of N_{ch} potassium (K^+) ionic channels is distributed. The stimulator is connected with the electrolyte bath at the inside (cytoplasm) and outside (extracellular electrolyte) of the cell through a pair of electrodes made of Silver/Silver–Chloride. Three main contributions to ionic current flow can be identified in the figure. The first contribution (A) is a membrane displacement current and the second contribution (B) is the leakage current sinked by the ionic channel [9]. The third contribution (C) is a current background noise accounting for the remainder of the cell membrane structure. The sum of these contributions constitutes the current measured by the VC tool, the contribution (C) being almost negligible in the more sophisticated PC technique. In view of a manageble mathematical modeling of the above system, we show in Fig. 2 its representation through lumped and distributed electrical equivalent parameters. The lumped parameters R_e and C_m are the electrolyte resistance R_e and the membrane capacitance, respectively. The former parameter accounts for ohmic losses due to the nonideal contact between electrodes and membrane, while the latter parameter accounts for the perfect insulator behaviour of the cellular membrane. Typical values of R_e and C_m are $\mathrm{M}\,\Omega$s and tenths of $\mathrm{f}\,F$, respectively. The distributed RC line embodies membrane background effects in a way that is similar to the Area-Contact model proposed in [5], while the remaining N_{ch} equivalent bipoles represent the effective

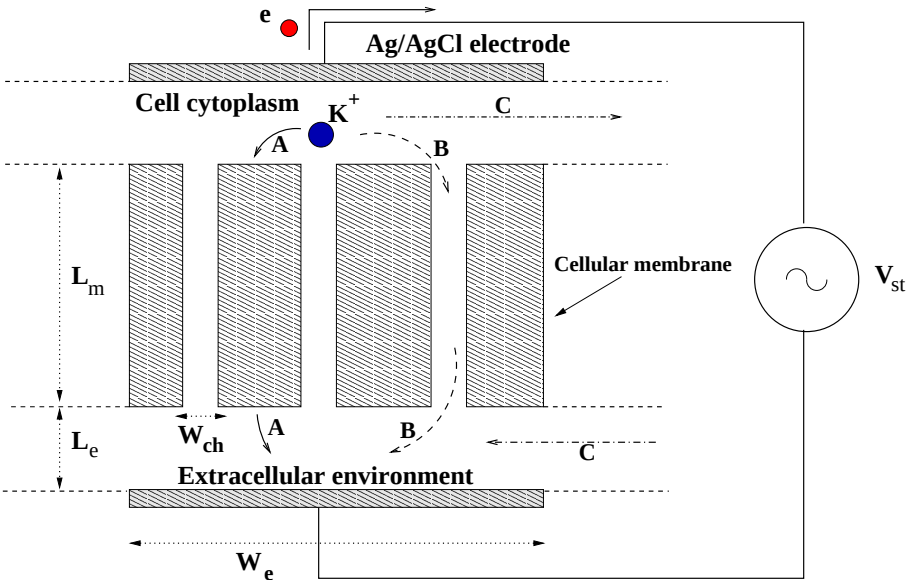

Figure 1: Schematic description of a voltage–clamp measurement system.

number of ionic channels that are directly stimulated by the voltage source V_{st}. The electrical equivalent characterization of these bipoles requires a detailed modeling of charge transport in each of the ionic channels. This can be done by adopting the Poisson-Nernst-Planck (PNP) system of partial differential equations (PDE) illustrated in Sect. 3 which accounts for the main electrochemical mechanisms driving ion flow throughout a channel [18, 17, 2]. In the case where N_{ch} gets large and/or there are several typologies of ionic channels, such a detailed modeling becomes computationally expensive and necessarily demands for the use of a reduced-order description. This can be done by a two-step procedure. The first step consists of performing an off-line simulation for each type of channel, based on the PNP differential model. The second step consists of extracting from the obtained results a suitable lumped electrical equivalent representation for the considered channel. The resulting reduced-order model, addressed in Sects. 3 and 5, is constituted by the system of ordinary differential equations (ODE), which is far cheaper than the full PDE-based approach and is ideally suited for an efficient and accurate description

of a bio-chip device through a multi-physics coupled model as discussed in [12], Chapt. 1, which is the ultimate goal of our ongoing research activity.

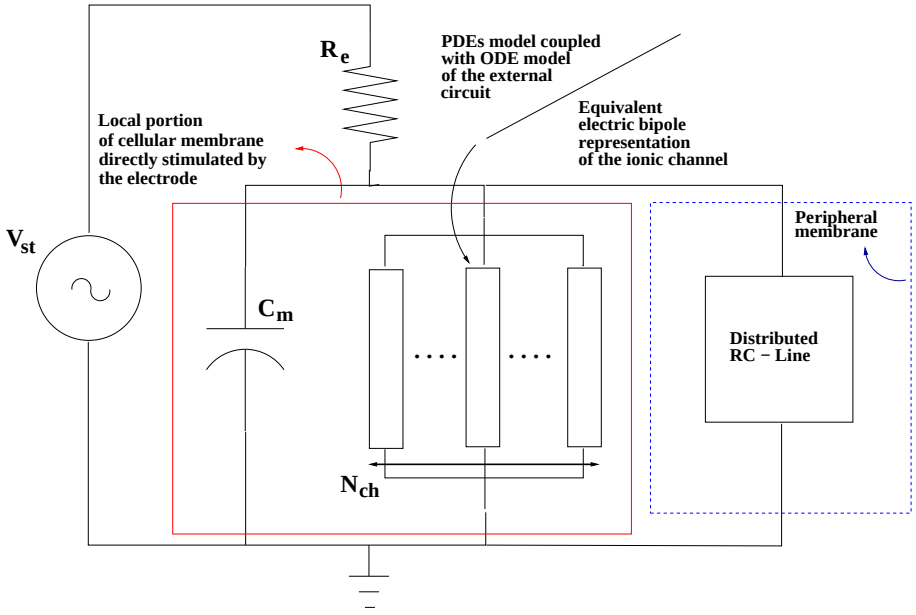

Figure 2: Equivalent electrical representation of a voltage–clamp measurement system.

3 Multi-Physics Mathematical Modeling Of Ionic Channels

In this section, we discuss a mathematical model based on a multi-physics approach to describe electrochemical transport phenomena in a single-species ionic channel and the interaction between the channel and the local surrounding environment. For this purpose, we consider in Sect. 3.1 the classical PNP partial differential model, and we characterize in Sect. 3.2 the system geometry as well as the boundary and initial conditions to be supplied to close the differential problem.

3.1 The PNP Partial Differential System

Electrochemical ionic transport phenomena in a single-species VOC can be described by the following Poisson-Nernst-Planck (PNP) system of partial differential equations [18, 17, 2]:

$$\begin{cases} \dfrac{\partial n}{\partial t} + \operatorname{div} \boldsymbol{J} = 0 \\ \lambda^2 \operatorname{div} \boldsymbol{E} = n + D \\ \boldsymbol{J} = (\mu \boldsymbol{E} + \alpha \boldsymbol{u}) n - \mu \boldsymbol{\nabla} n \\ \boldsymbol{E} = -\boldsymbol{\nabla} \varphi. \end{cases} \tag{1}$$

The variables of the system are the concentration n of the ionic species (which is assumed to be positively charged), the associated current density $\boldsymbol{J}$ and the electric field $\boldsymbol{E}$, that is related to the electric potential φ by $(1)_4$. The velocity of the electrolyte fluid $\boldsymbol{u}$ in $(1)_3$ is a given function, and in a more general mathematical picture, it is the solution of another partial differential system, the Navier-Stokes (NS) equations, which accounts for fluid-mechanical effects in the description of ionic transport in the channel. In the remainder of the article, the electrolyte fluid contribution will be neglected by setting $\boldsymbol{u} = \boldsymbol{0}$, and we refer the reader to [4, 12, 13] for a detailed discussion and numerical validation of the coupled PNP/NS model. The quantities μ and D are the ion mobility and a given function which represents a fixed concentration in the channel, respectively. We notice that a classical Drift-Diffusion-like constitutive equation is used for the current density $\boldsymbol{J}$ in $(1)_3$ (cf. [7]), with the addition of the term $\alpha \boldsymbol{u} n$ (α being a positive scaling constant), which acts as a correction to the drift term and is responsible for the coupling between electro–chemical forces and fluid–mechanical forces in (1). The parameter λ is the *scaled Debye length* [11] of the electrolyte, and is defined as

$$\lambda = \frac{\left(\dfrac{\varepsilon_e \overline{\varphi}}{q \overline{n}} \right)^{1/2}}{\overline{x}} \equiv \frac{l_e}{\overline{x}},$$

where $\overline{\varphi}$, $\overline{n}$ and $\overline{x}$ are the scaling factors for potential, concentrations and spatial coordinates,

respectively, while q and ε_e are the electron charge and the electrolyte permittivity, respectively. It is relevant to observe that if $\lambda^2 \ll 1$, the PNP system exhibits a singularly perturbed character (see [14]), and the corresponding solutions may exhibit internal and/or boundary layers, depending on the form of D and the given boundary conditions. In the problem at hand, a typical value of the above parameter is $\lambda^2 = 2 \cdot 10^{-2}$, which demonstrates that the PNP problem is singularly perturbed.

3.2 Geometry, Boundary and Initial Conditions

In this section, we define the computational domain and provide proper boundary and initial conditions for the PNP system. With this aim, Fig. 3 (left) shows a simplified geometrical description of a two–dimensional cross–section of a VOC, while Fig. 3 (right) shows the equivalent electrical representation of the physical system under investigation. In particular, V_{st} is the time-dependent applied voltage stimulation, R_e is the resistance accounting for ohmic contributions due to the cytoplasm electrolyte and the extracellular environment, and C_m is the capacitance accounting for charge accumulation across the membrane thickness due to the dielectrical behaviour of the membrane itself. From now on, we denote by $\Omega \subset \mathbb{R}^2$ the computational channel domain, and by Γ its boundary, with $\Gamma = \Gamma_1 \cup \Gamma_2 \cup \Gamma_3 \cup \Gamma_4$, and $\boldsymbol{n}_\Gamma$ the unit outward normal vector. For each boundary segment Γ_j, $j = 1, \ldots, 4$, an appropriate boundary condition can be imposed, according to either the user need or physical adherence. We also denote by $(t_{fin} - t_0)$ the (scaled) duration of the temporal evolution of system (1), t_0 being the starting time of the evolution, and in view of numerical time advancing, we partition the interval $[t_0,\, t_{fin}]$ into $N_T \geq 1$ time slabs of equal length $\Delta\, t = (t_{fin} - t_0)/N_T$.

The boundary and initial conditions that are considered in the present analysis of the PNP

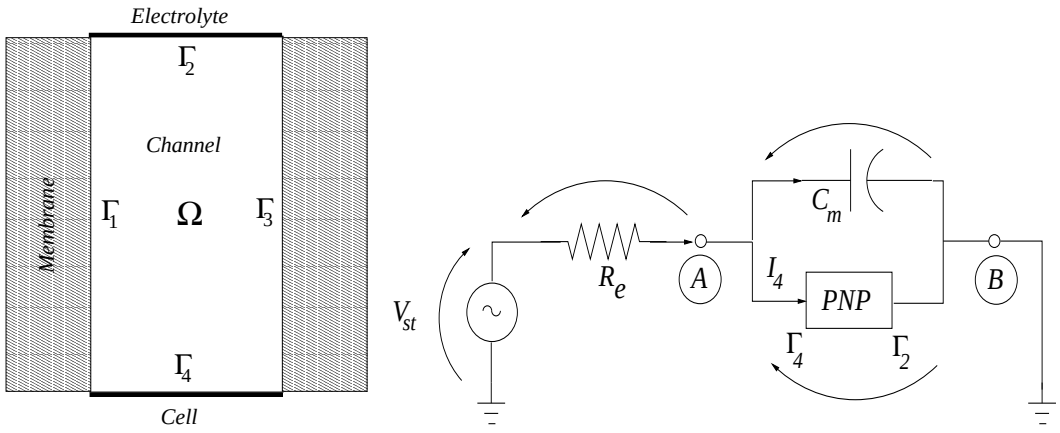

Figure 3: A two–dimensional geometrical description of a VOC (left). Equivalent electrical representation of the system comprising the ionic channel, the external stimulator, the membrane and the intracellular environment (right).

system (1) read as follows:

$$\begin{cases} \varphi(t) = 0 & \text{on } \Gamma_2 \\ \varphi(t) + R_e\, C_m \dfrac{d\varphi(t)}{dt} = V_{st}(t) - R_e\, I_4(t) & \text{on } \Gamma_4 \\ \boldsymbol{\nabla}\varphi \cdot \boldsymbol{n}_\Gamma = 0 & \text{on } \Gamma_1 \cup \Gamma_3 \\ n = \overline{n}_2 & \text{on } \Gamma_2, \\ n = \overline{n}_4 & \text{on } \Gamma_4, \\ \boldsymbol{J} \cdot \boldsymbol{n}_\Gamma = 0 & \text{on } \Gamma_1 \cup \Gamma_3, \\ n(\boldsymbol{x}, t_0) = n^0(\boldsymbol{x}) & \text{in } \Omega, \end{cases} \tag{2}$$

where $\overline{n}_i$ is the value of ion concentration on Γ_i, while $n^0(\boldsymbol{x})$ is the initial ion concentration in the channel at time $t = t_0$. With reference to Fig. 3 (right), condition $(2)_1$ states that node B is grounded, while condition $(2)_2$ is the result of the enforcement of the circuit Voltage Kirchoff Law (VKL), having defined

$$I_4(t) = W_{ch} \int_{\Gamma_4} \boldsymbol{J}(\boldsymbol{x}, t) \cdot \boldsymbol{n}\, d\gamma \qquad \forall t \in [t_0,\, t_{fin}],$$

and having assumed that the channel has a square cross-section in the direction perpendicular to the ionic flow axis of size W_{ch} (see Fig. 1). It is worth noting that condition $(2)_2$ amounts to solving an ordinary differential equation for $\varphi(t)$ at each time level. The numerical implementation of this latter procedure will be discussed in the nextcoming section. Conditions $(2)_{4-5}$ express the fact that a given concentration gradient is maintained across the channel, and conditions $(2)_3$ and $(2)_6$ express the fact that the channel is electrochemically self–contained. We notice that this latter condition can be easily generalized to include the possibility for an ionic current to flow (by osmosis) from the membrane into the ionic channel [4, 12, 13], thus increasing the portability of the model to other possible applications (for example, bio-hydraulics, micro-and-nano fluidics, plasma-dynamics, see [8]).

4 Functional Iterations and Numerical Approximation

In order to deal with the numerical approximation of the nonlinearly coupled PNP differential system discussed in the previous sections, we need to introduce a suitable iterative procedure which allows the successive solution of the model equations. Then, proper finite element formulations must be used for the discretization of the resulting decoupled differential subproblems.

4.1 A Staggered Algorithm

The staggered algorithm for the successive solution of the PNP system proceeds as indicated in the flowchart of Fig. 4. For each time level t_m, $m = 0, \ldots, N_T - 1$, the following steps are performed, for each $k \geq 0$:

(a) solve the PNP system with a given voltage $\varphi^{(k)}$ on Γ_4. This provides in output the updated ion concentration $n^{(k+1)}$ and electric field $\boldsymbol{E}^{(k+1)}$, and, in turn, the current $I_4^{(k+1)}$;

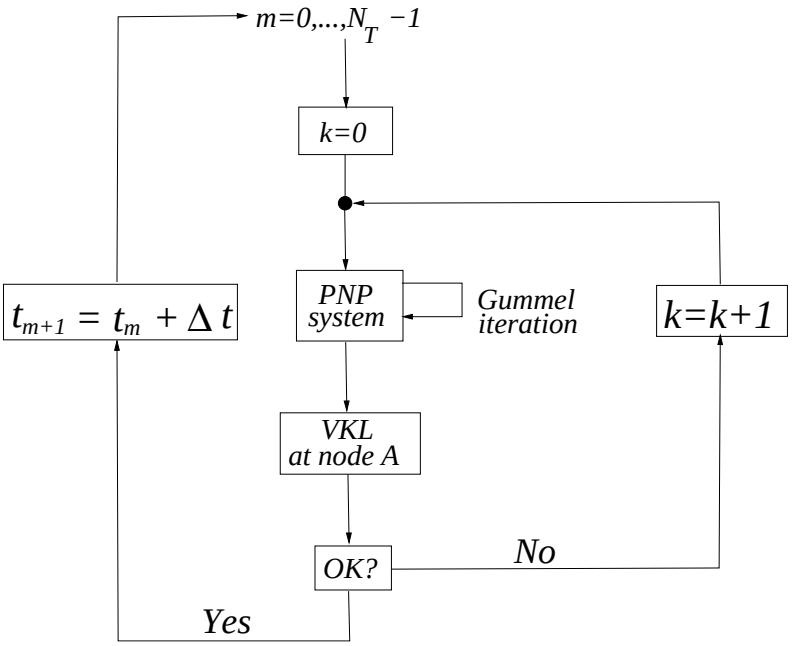

Figure 4: Flow-chart of the staggered iteration.

(b) use the VKL $(2)_2$ to compute the updated value $\varphi^{(k+1)}$ of the potential of node A

$$\frac{V_{st}(t_{m+1}) - \varphi^{(k+1)}(t_m)}{R_e} = I_4^{(k+1)}(t_m) + C_m \frac{\varphi^{(k+1)}(t_m) - \varphi(t_m)}{\Delta t};$$

(c) compare the voltage increment with a specified input tolerance `toll`

$$\left|\varphi^{(k+1)}(t_m) - \varphi^{(k)}(t_m)\right| < \texttt{toll} \qquad k \geq 0; \tag{3}$$

(d) let k^* be the value of k at which (3) is satisfied for the time level t^m. Then, set

$$n(\boldsymbol{x}, t_{m+1}) = n^{(k^*)}(\boldsymbol{x}, t_m), \qquad \varphi(\boldsymbol{x}, t_{m+1}) = \varphi^{(k^*)}(\boldsymbol{x}, t_m)$$

and set $t = t_{m+1}$.

Step (a) is carried out by resorting to a suitable linearization of the PNP system, through the classical Gummel's map that is widely employed in contemporary semiconductor device simulation (see [7] for a detailed description of the algorithm and for the analysis of its convergence properties).

4.2 Finite Element Approximation

As previously anticipated, the solutions of the PNP subsystem can exhibit a markedly singularly perturbed character (see [7]). Moreover, due to the common structure in divergence form of $(1)_{1,2}$, conservation of fluxes (electric field and current density) is an important issue for the computed solution. As a matter of fact, it is well–known that flux post–processing may lead to a degradation in the accuracy, due to numerical differentiation. Moreover, standard displacement–based finite element formulations do not provide interelement continuity of normal flux, which constitutes a violation of the action–reaction principle on the discrete level. Therefore, in view of the finite element approximation of the PNP system, we use the Exponentially Fitted Mixed Finite Volume scheme proposed and analyzed in [15] and further investigated in [3]. The most relevant features of this finite element formulation are that it is locally conservative and it satisfies a discrete maximum principle. This latter property ensures that the computed approximate ion concentration is a strictly positive function under the sole request that the computational grid is of Delaunay type, this latter condition allowing the presence of obtuse triangles in the geometrical partition of the domain. The numerical performance of the discretization scheme in the simulation of VOCs are extensively discussed in [4, 12, 13].

5 Numerical Results

In this section, we discuss a selection of significant test cases, which demonstrate how the modeling strategies outlined in Sects. 2 and 3 can be profitably employed for the simulation of a realistic VOC subject to a measurement procedure, with an optimal trade-off between accuracy and computational effort. In all the performed computations, we assume that the external

voltage stimulation has the following form

$$V_{st}(t) = V_N + \Delta V u(t - t_{st}), \tag{4}$$

where V_N is the Nernst potential typical of the K^+ channel, $u(\cdot)$ is the unit step function, and $t_{st} > t_0$ is the time level at which a voltage drop equal to ΔV is applied across the membrane. We also set $t_0 = 0$, $N_T = 20$ and $t_{st} = t_0 + 2\Delta t$, while the values of the parameters ΔV and Δt are specified for each simulation. The computational domain Ω is a rectangle as in Fig. 1 with $L_m = 10nm$ and $W_{ch} = 1nm$, while the finite element grid consists of 288 triangles. The initial condition for the ionic concentration in the channel is $n^0(\boldsymbol{x}) = n_{V_N}(\boldsymbol{x})$, where n_{V_N} represents the ion concentration at the Nernst equilibrium condition.

5.1 Test Case With Ideal Voltage Stimulation

In this section, we consider a simulation test case that represents an example of the two–step procedure proposed in Sect. 2. The off-line computations, based on the PNP partial differential model, needed to extract an equivalent electric lumped parameter model are performed under the assumption of an ideal simulation. Referring to Fig. 3 (right), this means that the electrode shortcuts the resistive path R_e, stimulating directly node A. Such a situation corresponds to placing the electrode in contact with the cellular membrane, which amounts to setting $L_e = 0$ in Fig. 1 and $R_e = 0$ in $(2)_2$. A first simplified scheme of the equivalent electric model is illustrated in Fig. 5. The equivalent capacitance C_{eq}, which accounts for the accumulation/depletion of ions during the current transient, is defined as

$$C_{eq} = \frac{\Delta Q}{\Delta V},$$

with $\Delta Q = \int_{t_{st}}^{t_{fin}} (I_4(\tau) - I_2(\tau))\, d\tau$, I_4 and I_2 being the currents flowing across the cross-sections Γ_4 and Γ_2 of the channel. The purely resistive load R_{eq} exhibited by the channel in stationary

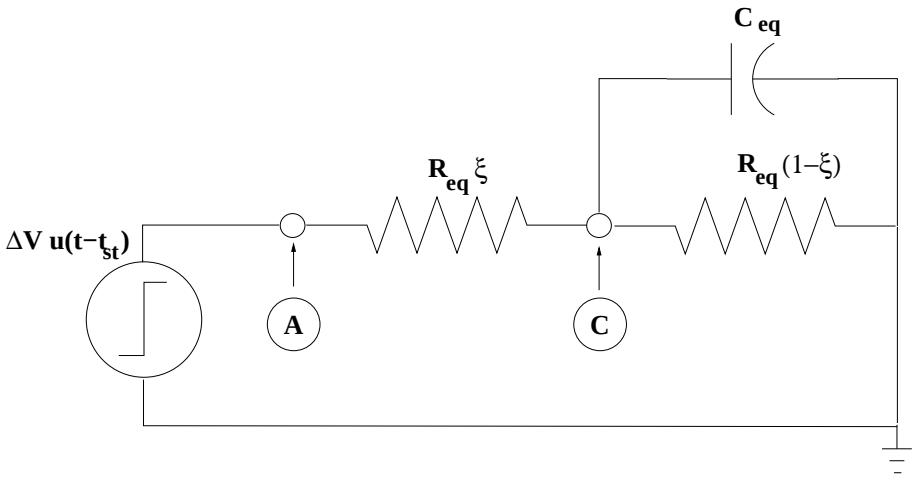

Figure 5: Equivalent electric model of the channel.

conditions is computed as

$$R_{eq} = \frac{\Delta V}{I_4(t_{fin})}.$$

In view of transient simulations, R_{eq} is partitioned into two contributions by introducing the adimensional parameter ξ, as illustrated in Fig. 5. This latter parameter is tuned up in such a way that the solution of the ODE model of the equivalent electrical circuit agrees with the current transient computed with the PDE off–line simulation.

Such parameter extraction procedure is carried out in the case $\Delta V = 250mV$ and $\Delta t = 500ps$, as shown in Fig. 6. The circular markers identify the ionic current obtained by solving the PNP problem, with a solid line to interpolate the computed current values. The cross markers represent the transient current predicted by the equivalent ODE model, having set $C_{eq} = 0.28\,\mathrm{a}F$, $R_{eq} = 9.61\,\mathrm{G}\Omega$ and $\xi = 0.19$. Defining by $I_{AC}(t)$ the current flowing from node A to node C and computed by the ODE model (cf. Fig. 5), the maximum discrepancy, in absolute value, between $I_4(t)$ and $I_{AC}(t)$ over the time interval of the simulation is of the order of $5pA$, which corresponds to an accuracy of the reduced-order model with respect to the full-

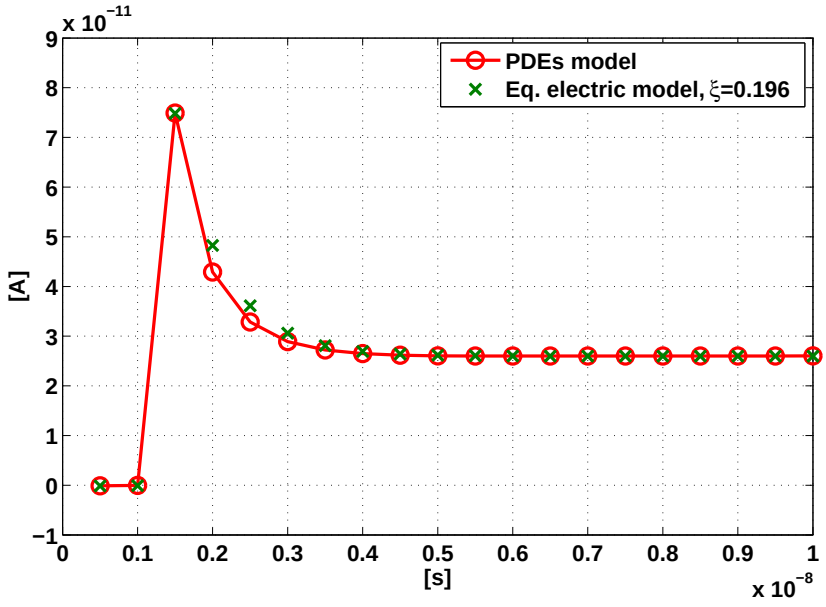

Figure 6: Transient behaviour of the ionic current in the case $\Delta V = 250mV$.

scale PNP model of about 90 percent. This obtained accuracy is a very good result, compared with the extreme simplicity of the electrical equivalent lumped parameter approximation that is employed. A second numerical experiment similar to the previous one is illustrated in Fig. 7 in the case of a negative voltage biasing drop $\Delta V = -150mV$ applied to the channel. The time step Δt is the same as in the previous test case, while the electrical equivalent parameters are $C_{eq} = 0.17\,\mathrm{a}F$, $R_{eq} = 19.47\,\mathrm{G}\Omega$ and $\xi = 0.08$. The accuracy of the ODE model is the same as computed in the case where the voltage drop is equal to $\Delta V = 250mV$.

5.2 Test Case With Non-Ideal Voltage Stimulation

In this section, we consider a more realistic measurement experiment, accounting for non–ideal effects such as ohmic losses in the electrolyte bath. These latter are well–known to be responsible for a slower current transient, because they limit the ability of the electrode to instantaneously provide all of the ionic charge needed by the cellular membrane [9]. Referring to Fig. 1, we set

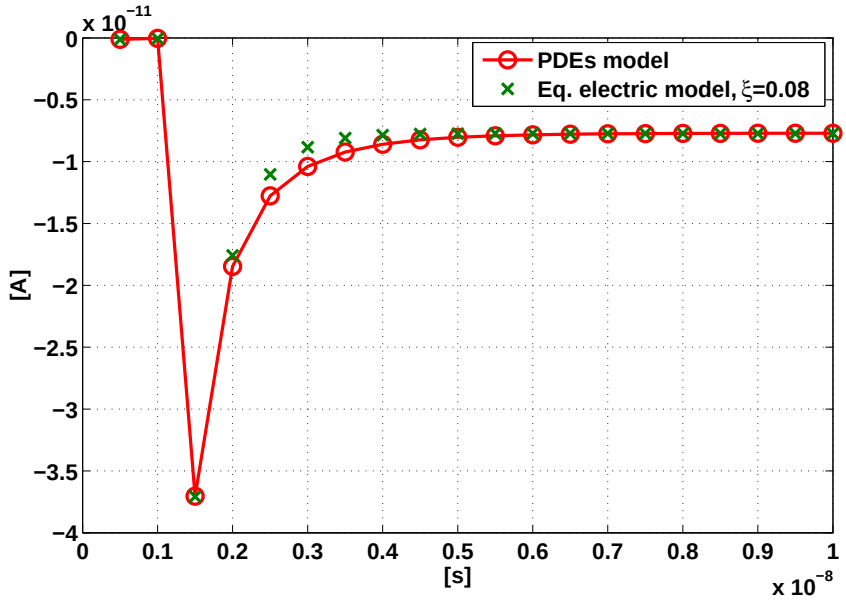

Figure 7: Transient behaviour of the ionic current in the case $\Delta V = -150mV$.

$W_e = 1\mu m$, which corresponds to an electrode of surface $A_e = 1\mu m^2$, and $L_e = W_e$. Noting that the specific capacitance $C_{m,s}$ per unit area of the membrane is of the order of $1\mu F\, cm^{-2}$ (see [10]), the capacitive load exhibited by the cellular membrane is $C_m = C_{m,s}\, A_e = 10\mathrm{f}F$. We set also $R_e = 7\mathrm{M}\Omega$, having assumed a resistive path of length L_e and cross–section A_e. The time step chosen for the simulation is $\Delta t = 20ns$, while $\Delta V = -150mV$. Fig. 8 shows the time evolution of the total current provided by the electrode, while Fig. 9 represents the time evolution of the current sinked by the ionic channel. The current peak at the beginning of the transient is due to the displacement current contribution (A) (cf. Fig. 1) and is almost three orders of magnitude larger than the steady-state current sinked by the ionic channel (cf. Fig. 9). The equivalent time constant of the transient phenomenon can be roughly estimated as $\tau_{eq} = R_e\, C_m \simeq 70ns$, and can be compared with the time scale of the current dynamics in the case of an ideal stimulation, confirming that the transient duration is dominated by the displacement current contribution, as anticipated above.

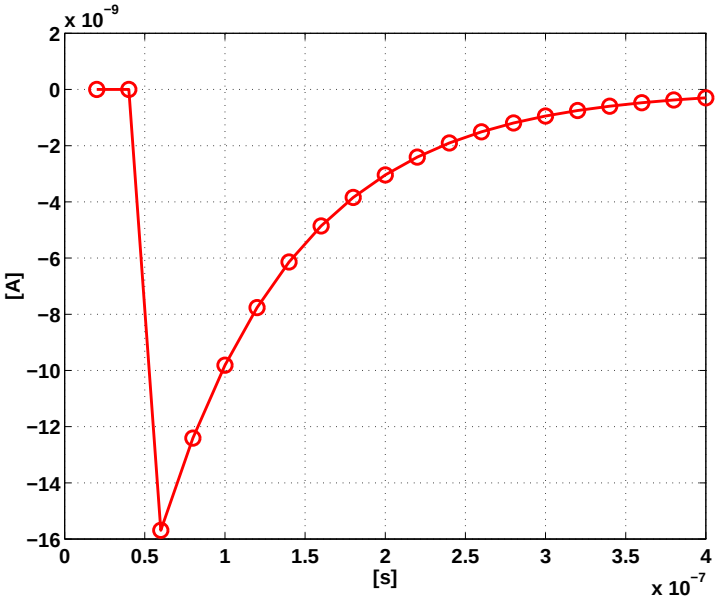

Figure 8: Total current provided by the electrode.

A concluding test case is carried out in the following to check the effect of the presence of a large number of ionic channels involved in the measurement process on the overall simulation of the biological system. In such a realistic case the use of the equivalent electrical model discussed in Sect. 5.1 is strongly recommended in order to reach an optimal trade-off between modeling accuracy and computational effort. With this purpose, under the simplifying assumption that all the channels are identical from the structural point of view, we can still employ the boundary conditions described in Sect. 4 by modifying Eq. $(2)_2$ as

$$\varphi(t) + R_e\, C_m \frac{d\varphi(t)}{dt} = V_{st}(t) - R_e\, N_{ch}\, I_4(t), \tag{5}$$

in order to account for the amplification equal to a factor N_{ch} of the single current contribution I_4. Fig. 10 illustrates the time evolution of the voltage drop across the membrane in the case $N_{ch} = 1000$. Notice that the effective applied voltage stimulation across the mebrane is $40\,mV$ lower than the external voltage drop $\Delta V = -150mV$ because of the significant ohmic loss

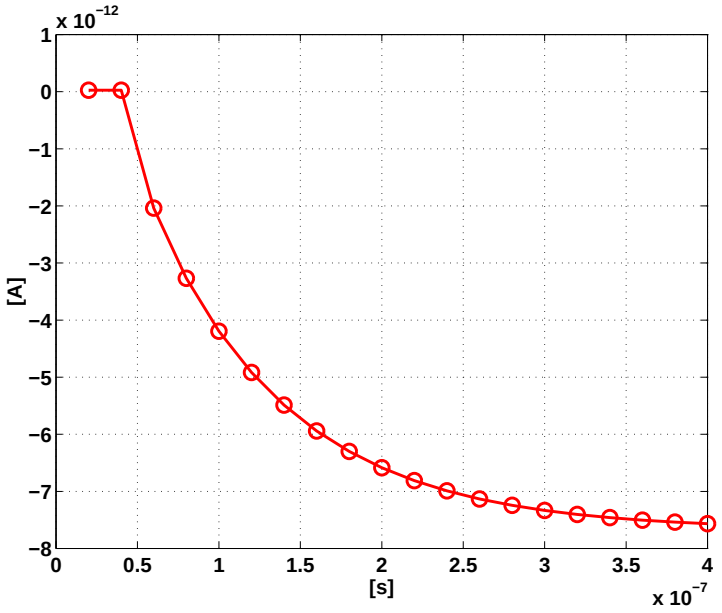

Figure 9: Ionic current sinked by the channel.

introduced, in the present case, by the electrolyte resistive path R_e.

6 Conclusions and Future Perspectives

In this article, we have addressed the mathematical modeling and simulation of a measurement procedure for voltage operated ionic channels.

With this aim, a partial differential system of equations has been proposed to describe charge transport in the channel, and the model has been coupled to the external stimulator equipment through the introduction of proper boundary conditions for the electric potential across the channel membrane.

The PDE model has then been employed to derive an equivalent reduced-order model for the electrical representation of the channel by means of simple lumped parameters.

Extensive numerical experiments have been performed to compare the accuracy of the full

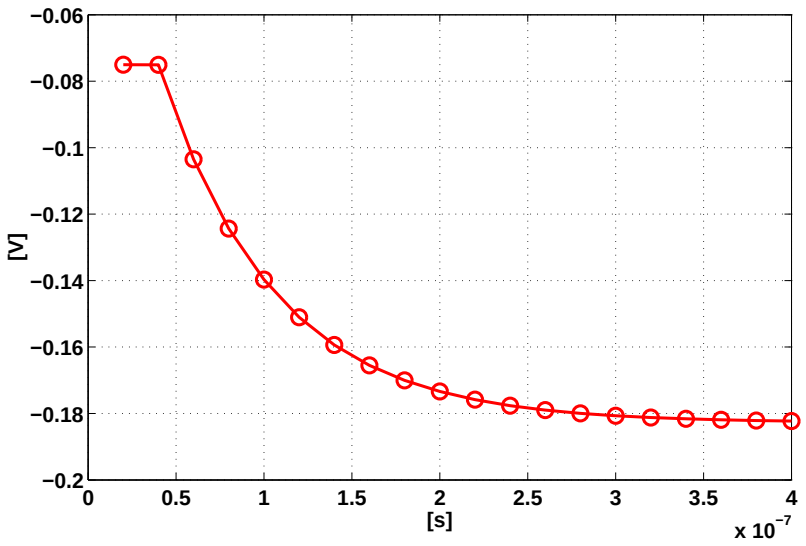

Figure 10: Voltage drop across the membrane in the case $N_{ch} = 1000$.

PDE model with that of the reduced-order model on the simulation of ionic channels subject to ideal and non-ideal stimulations.

Further research directions that we aim to investigate in the framework of measurement applications in ElectroPhysiology are:

- the improvement of the extraction procedure of equivalent electrical parameters by accounting for the specific biological, electrochemical and geometrical properties of the considered channel;
- the implementation of a mixed-mode simulation tool based on the coupling between the PDE and ODE differential models, in order to study more complex physical situations such as gating phenomena and action potentials [6];
- the use of the mathematical modeling and computational techniques discussed above for the accurate and efficient simulation of the Patch Clamp measurement equipment.

7 Acknowledgements

The authors gratefully thank Dr. Giovambattista Marino for his contribution to the research object of the manuscript. Massimo Longaretti was supported by the Grant "Modelli Computazionali in Nano-Bio-Elettronica", Politecnico di Milano (2007). Joseph W. Jerome was supported by ONR Subcontract LLCN00014-05-C-0241 (Advanced Tools for Computational Materials Engineering). Riccardo Sacco was supported by the M.U.R.S.T. Grant "Approssimazione Numerica di Problemi Multiscala e Multifisica con Tecniche Adattive" (2006–2008).

References

[1] B. Alberts, A. Johnson, J. Lewis, M. Raff, K. Roberts, and P. Walter. *Molecular Biology of the Cell.* Garland Publishing, New York, 2002.

[2] V. Barcilon, D. Chen, R. Eisenberg, and J.W. Jerome. Qualitative properties of steady-state Poisson-Nernst-Planck systems: perturbation and simulation study. *SIAM J. Appl. Math.*, 57 (3):631–648, 1997.

[3] F. Brezzi, L.D. Marini, S. Micheletti, P. Pietra, R. Sacco, and S. Wang. Discretization of semiconductor device problem (i). In P.G. Ciarlet, W.H.A. Schilders, and E.J.W. ter Maten, editors, *Handbook of Numerical Analysis*, volume 13, pages 317–441. Elsevier North-Holland, Amsterdam, 2005.

[4] B. Chini, J.W. Jerome, and R. Sacco. Multi-physics modeling and finite element approximation of charge flow in ionic channels. In L.J. Ernst, G.Q. Zhang, P. Rodgers, M. Meuwissen, S. Marco, and O. de Saint Leger, editors, *Proceedings of EUROSIME06 Conference, Como,*

Italy, pages 153–160, Maastricht (The Netherlands), April 24 2006. IEEE Shaker Publishing.

[5] P. Fromherz. Neuroelectronics interfacing: Semiconductor chips with ion channels, cells and brain. In R. Weise, editor, *Nanoelectronics and Information Technology*, pages 781–810. Wiley-VCH, Berlin, 2003.

[6] B. Hille. *Ionic Channels of Excitable Membranes*, volume 17(1). Sinauer Associates, 1992.

[7] J.W. Jerome. *Analysis of Charge Transport*. Springer-Verlag, Berlin Heidelberg, 1996.

[8] G. Karniadakis, A. Beskok, and N. Aluru. *Microflows and Nanoflows. Fundamentals and Simulation*, volume 29 of *Interdisciplinary Applied Mathematics*. Springer–Verlag, New York, 2005.

[9] U.B. Kaupp and A. Baumann. Neurons–the molecular bases of their electrical excitability. *Nanoelectronics and Information Technology*, pages 147–164, 2003.

[10] J. Keener and J. Sneyd. *Mathematical Physiology*, volume 8 of *Interdisciplinary Applied Mathematics*. Springer–Verlag, New York, 1998.

[11] C. Kittel. *Introduction to Solid State Physics*. Wiley, 1956.

[12] M. Longaretti and G.Marino. Coupling of electrochemical and fluid-mechanical models for the simulation of charge flow in ionic channels. Master's thesis, Politecnico di Milano, Milan, 2006.

[13] M. Longaretti, G. Marino, B. Chini, J.W. Jerome, and R. Sacco. Computational models in nano-bio-electronics: simulation of ionic transport in voltage operated channels. Technical

report, Dipartimento di Matematica "F. Brioschi", Politecnico di Milano, 2006. To appear in Jour. Nanosc. Nanotech. (2007).

[14] P.A. Markowich. *The Stationary Semiconductor Device Equations*. Springer-Verlag, Wien-New York, 1986.

[15] S. Micheletti, R. Sacco, and F.Saleri. On some mixed finite element methods with numerical integration. *SIAM J. Sci. Comput.*, 23-1:245–270, 2001.

[16] E. Neher. Molecular biology meets microelectronics. *Nature Biotechnology*, 19:114, 2001.

[17] J.H. Park and J.W. Jerome. Qualitative properties of steady-state Poisson-Nernst-Planck systems: mathematical study. *SIAM J. Appl. Math.*, 57 (3):609–630, 1997.

[18] I. Rubinstein. *Electro–Diffusion of Ions*. SIAM, Philadelphia, PA, 1990.

[19] B. Straub, E. Meyer, and P. Fromherz. Recombinant maxi-k channels on transistor, a prototype of iono-electronic interfacing. *Nature Biotechnology*, 19:121–124, 2001.